Journal of the Korea Institute for Structural Maintenance and Inspection
Vol. 26, No. 3, June 2022, pp.48−54
https://doi.org/10.11112/jksmi.2022.26.3.48

pISSN 2234−6937
eISSN 2287−6979

Stiffness Degradation Induced by Seismic Loading on a RC Shear Wall

Yun Lee[1*]

지진하중에 의한 철근콘크리트 전단벽의 강성 저하에 관한 연구

이윤[1*]

Abstract: This research describes a quantitative procedure used to estimate the effect of concrete cracking on stiffness degradation of concrete shear walls and provides analytical references for the seismic design of concrete shear walls. As preliminary research on the seismic response of concrete shear walls, nonlinear transient analysis was performed with commercial FE software. The study presents the nonlinear time history analysis results in terms of concrete damage and cracking behavior induced by seismic input motions. By varying the input motions, concrete strength and shear wall thickness, the seismic responses of a shear wall were examined with nonlinear time history analysis, and the progressive cracking behavior and corresponding hysteresis loop were described. Based on the analysis results, frequency and stiffness degradation of the shear wall from progressive concrete damage and cracking were captured with respect to the seismic levels. The results of this study suggest that stiffness degradation from concrete cracking should be appropriately considered when determining the seismic capacity of RC shear wall structures.

Keywords: Seismic loading; Reinforced concrete; Shear wall; Finite element analysis; Concrete crack

1. Introduction

Because seismic design has become increasingly more important recently for nuclear power plants, the American Society of Civil Engineers (ASCE) compiled the ASCE 43-05 report (ASCE/SEI 43, 2005) asserting that there is a need to assess nuclear power plant structures taking into consideration the impact of latent cracks, and it was also reported by the American Concrete Institute (ACI) that cracking reduces the stiffness of a structural member, and cracking should be considered in stiffness assumptions so that drift caused by wind or earthquakes is not grossly underestimated (ACI 349, 2001).

Additionally, the U.S. Nuclear Regulatory Commission (US NRC) also mandated that project owners should design a new nuclear power plant taking into consideration the impact of latent cracks. Accordingly, based on the above assertions and requirements for evaluating nuclear power plant safety, the impact of latent cracks has been recognized to be an important factor as seen in the AP1000 and US-APWR examinations for obtaining the U.S. design certificate (DCD, 2011; Arel et al., 2017; NUREG/CR 6926, 2007; Sogbossi et al.,2017; US-APWR, 2011; Wang et al., 2018). On the other hand, when experimentally verifying a rectangular box-shaped shear wall system tested under the JNES/NUPEC program in Japan, it was reported that the frequency and shear stiffness of a shear wall decreased with an increase in the seismic loading history (Choubey et al., 2014; Habasaki et al., 1999; Hiroshi et al., 2001; Kusama et al., 2003; Mistri et al., 2016; Shojaei et al., 2017; Syed et al., 2015; Torita et al., 2004; Zhou et al., 2018).

Thus, the aim of this study was to analytically identify the phenomenon of stiffness reduction caused by the presence of latent cracks brought about by seismic loads in the shear walls of reinforced concrete structures. The reinforced concrete shear wall was selected in this study because it is a major structural member used extensively in all Nuclear Power Plants to provide seismic load resisting capability.

In this study, seismic time history analysis was carried out on RC shear walls to investigate the impacts of cracks on structures with nonlinear finite element analysis. To quantitatively reflect the influence of cracks on a seismic design, the influence of the cracks according to the level of the seismic load was investigated in terms of the natural frequency and shear stiffness by classifying the possible seismic loads by grade.

[1]정회원, 대전대학교 토목환경공학과 교수
***Corresponding author:** yunis@dju.kr
Department of Civil Engineering, Daejeon University, Daejeon, 34520, Korea
•본 논문에 대한 토의를 2022년 7월 31일까지 학회로 보내주시면 2022년 8월호에 토론결과를 게재하겠습니다.

By varying the input motions, concrete strength and shear wall thickness, the seismic responses of the shear wall were considered with nonlinear time history analysis, and the progressive cracking behavior and corresponding stiffness degradation were investigated.

The paper is organized into four sections. Section 1 is the introduction, and Section 2 provides a brief description of the numerical framework used in this study. The cracking and failure description, the numerical results of an individual time history analysis and their comparisons are discussed in Section 3. Finally, conclusions are provided in Section 4.

2. Numerical Framework for the Nonlinear Analysis of a Shear Wall

2.1 Preparation of Numerical Analysis

2.1.1 Finite element analysis program

To identify the shear stiffness degradation behavior from concrete cracks, the numerical analysis should first adopt real earthquake data and carry out a nonlinear time history analysis. It should also be able to effectively simulate cracks generated in a concrete structure by seismic loads. To this end, this study selected ANSYS V.13.5 which is the common software used to do a nonlinear time history analysis. Because cracks in concrete should be simulated throughout the whole analysis process, the appropriate material model should be used for an applied finite element program when considering concrete cracks. ANSYS V.13.5 provides SOLID65 as a material model for concrete which can take into consideration different damages and cracks in concrete. Accordingly, this study selected SOLID65 from the ANSYS V.13.5 software as the material model for concrete which can simulate gradual damages and cracks in concrete.

2.1.2 Mesh modeling of a shear wall

In this analysis, an RC shear wall structure, for which a vibration test was successfully done shown in Fig. 1, was selected as the analysis target. Based on the specification of the selected shear wall and the details of the reinforcing bars, mesh modeling was done on a target, and the reinforcing bars in shear wall and the flange were the modeled structure shown in Fig. 2. Additionally, the bottom of the shear wall was fixed with an assigned boundary condition. To reflect the effect of the vertical load on the shear wall, a stress of 0.442 MPa was vertically loaded onto the top surface of the shear wall, and a mass of 50 tonf was given to the mass center of the vertical load using the point mass function of ANSYS V.13.5 to reflect the effect of mass on the top of the shear wall. The concrete shear wall was modeled with SOLID65, an eight-node solid element, provided by ANSYS, and the reinforcing bars were modeled with the LINK180 element, a two node truss element.

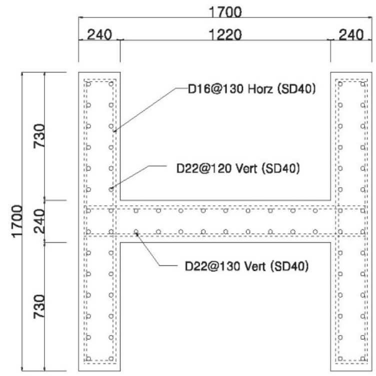

Fig. 1 Shear wall configuration and dimensions of the Rebar Configuration (Unit: mm)

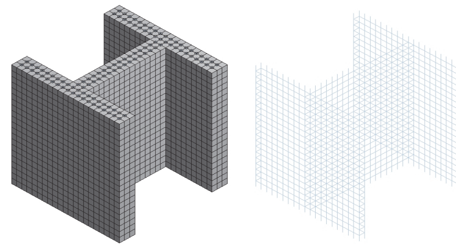

Fig. 2 Mesh model and rebar configuration

2.1.3 Concrete material model

In cases in which a cyclic load such as a seismic load should be simulated with the nonlinear behavior of concrete, analysis programs are generally designed to enable a concrete material model to represent the gradual degradation of stiffness and strength using a damage model for which the tangent modulus of elasticity decreases according to the stress history. Generally, existing cracks in a structure influence the stiffness and strength of a structure and change the various aspects of failure, which should be appropriately described in the numerical model. This study used SOLID65 from ANSYS V.13.5 as a numerical model to simulate damage effects caused by concrete cracks. SOLID65 can effectively simulate a multi-axial cyclic history behavior, and adopt a smeared crack approach to simulate concrete cracks to be considered in this study. The smeared crack model can be easily engrafted on a finite element method and has the advantage of overcoming the greatest weaknesses of a discrete crack model in which crack initiation and propagation have to be determined beforehand. A smeared crack model can represent the effects of cracks by changing the material constitutive relations through a uniform distribution of cracks inside a finite element. With the implementation of SOLID65, the crack occurrence in a concrete shear wall can be visually identified in the post-process provided by ANSYS V.13.5, and the cracking patterns according to an increasing seismic load can be investigated in this study.

2.1.4 Applied load

As a basic input motion, the time-acceleration history, in which the maximum acceleration is scaled to 0.3 g, the safe shutdown earthquake (SSE) value, is implemented shown in Fig. 3. The time interval and its time duration are 0.01second and 24 seconds, respectively. The minimum time increment in the time history analysis was adopted based on 1/10 of the natural period known as the stability limit of dynamic analysis. The natural frequency of a given shear wall structure was assessed approximately at 23 Hz through modal analysis, and the minimum time increment was considered as 0.004 seconds smaller than 0.0043 seconds which is estimated as the stability limit of the dynamic analysis.

2.2 Classification of the Performed Numerical Analysis

The purpose of this study was to identify the influence of concrete cracks inside a shear wall structure with a relatively low tensile strength under a small to large seismic load on the stiffness reduction of a structure. To this end, the numerical cases done by this study are summarized as follows:

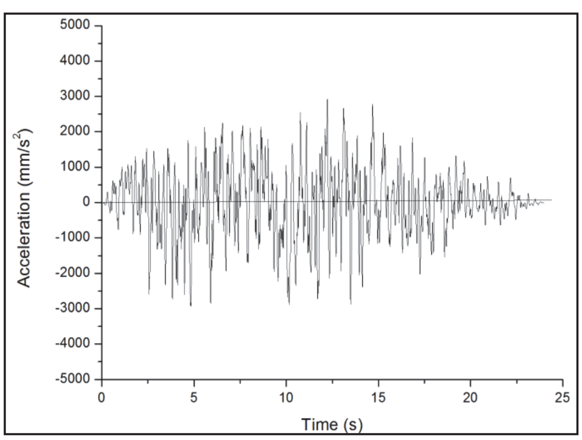

Fig. 3 Basic input motion scaled to a PGA of 0.3 g

2.2.1 Modal analysis

Modal analysis was done on a RC shear wall for a concrete strength of 21MPa modeled as mentioned in section 2.1 using ANSYS V.13.5. Because a concrete shear wall shows nonlinear behavior due to the nonlinearity of the concrete itself, natural frequency according to modal analysis is not the same as the natural frequency of a concrete shear wall; however, based on this fact, the modal analysis of a shear wall in an elastic state was done to determine the time interval and appropriate mesh size in the time history analysis by assessing the natural frequency and mode of a shear wall not taking into account the nonlinear effect.

2.2.2 Static analysis

The main scope of this study was to identify the seismic behavior of RC shear walls through a dynamic analysis. However, an analysis of a static loading case in lateral displacement on a target member was conducted to predict the cracking load and ultimate load of a target shear wall and to compare them with dynamic loading cases. The static analysis was done and designed to be compared with a hysteresis curve under a dynamic analysis.

2.2.3 Increasing seismic load cases for RUN-1 ~ RUN-5

Based on basic input motions, a nonlinear time history analysis for an earthquake duration up to 24 seconds was conducted by scaling peak ground acceleration (PGA) for a concrete strength of 21 MPa from RUN-1 to RUN-5 for 5 phase loads, 0.1, 0.2, 0.3, 0.5 and 0.7 g, shown in Fig. 4. Through this analysis, the overall pattern and extent of concrete cracks are identified, and the dynamic features of a shear wall under a seismic load is identified through an FFT analysis with a maximum response.

3. Analysis Results and Discussion

3.1 Modal Analysis

As described in section 2.2.1, modal analysis was conducted to determine the size of the elements for mesh modeling and to analyze the frequency in an elastic state. Fig. 5 shows the mesh configuration for a concrete strength of 21 MPa. According to the analysis results, when the size for an element of concrete was 40 mm, the natural frequency of direction Z, which is the direction of an input earthquake, was 22.55 Hz, and when the

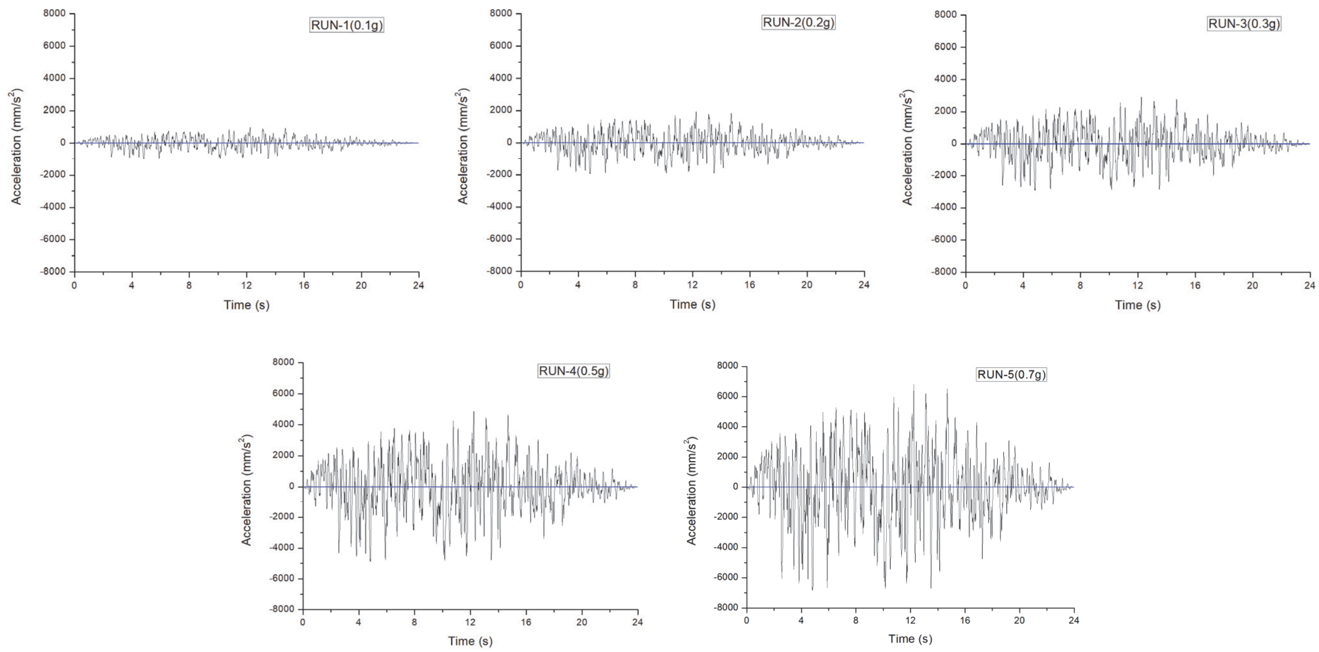

Fig. 4 Increasing seismic load cases

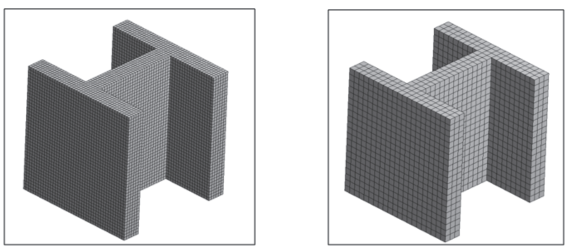

(a) Mesh size: 40 mm, 28728 elements

(b) Mesh size: 80 mm, 3591 elements

Fig. 5 Comparison of mesh configurations via modal analysis

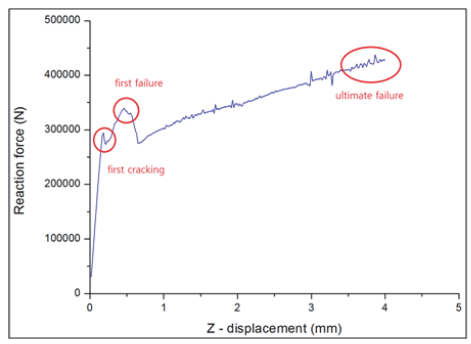

Fig. 6 Load-displacement curve from a static analysis on the concrete strength of 21 MPa

element size was 80 mm, which is about three times the maximum size of the aggregate, the natural frequency was 22.57 Hz. It was observed that there was little difference in the natural frequency according to the size and number of element. Considering analysis time saving and computer memory capability, the mesh size was determined as 80 mm, and the relevant numerical analysis was conducted.

3.2 Static analysis

Fig. 6 shows a load-displacement curve derived from a static analysis for a concrete strength of 21MPa. The first cracking load after loading was 0.294 MN; the local maximum load was 0.339 MN, and the ultimate failure load was 0.428 MN. By investigating the load that generates cracks and the ultimate failure load through static analysis, the magnitude level of the seismic load for the increasing load cases in section 2.2.3 was determined. Fig. 7 shows a cracking pattern after placing a static load. It was found that typically, diagonal cracks occur in

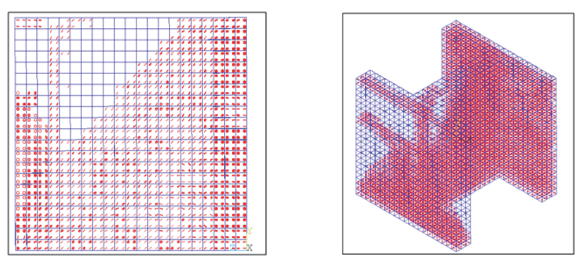

Isometric view

Side view of the shear wall plan

Fig. 7 Cracking pattern from a static analysis on the concrete strength of 21 MPa a concrete shear wall which confirm that the failure of a concrete shear wall, which is the target of this study, is controlled by the shear failure mode at the ultimate state.

3.3. Increasing seismic load cases for RUN-1 ~ RUN-5

As mentioned in section 2.2.3, a nonlinear time history analysis was conducted based on gradually increasing the magnitude of the seismic load from RUN-1 through RUN-5 for a concrete strength of 21 MPa (modulus of elasticity of 20 GPa; tensile strength of 1.5 MPa) Figs. 8 to 12 show the acceleration response at the top surface of a shear wall by each phase in the frequency domain using Fast Fourier Transform (FFT) and the load-displacement curve after an individual time history analysis.

According to the load-displacement curve in Fig. 8, energy loss hardly occurred due to the applied load, and stiffness reduction also was hardly caused by the cyclic loading history. Moreover, concrete cracking did not occur according to the numerical analysis result. In the case of RUN-2 with a PGA of 0.2 g in Fig. 9, the maximum load was about 0.15 MN, which is equivalent to about 50% of the first cracking load of 0.294 MN for the static loading case. This means that concrete cracking and the ensuing stiffness reduction hardly occurred.

In the case of RUN-3 with a PGA of 0.3 g, as shown in Fig. 10, the energy loss and stiffness reduction according to the cyclic loading history in the load-displacement curve were caused by concrete cracking at the bottom of the shear wall and flange. The maximum load was about 0.2 MN, which is equivalent to about 60% of the first cracking load of 0.294 MN for the static loading case.

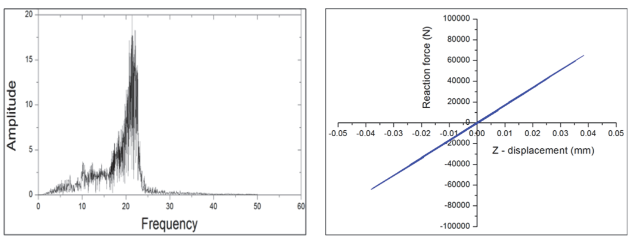

(a) FFT result (b) Load-displacement curve

Fig. 8 Results of seismic analysis for phase load RUN-1 on a concrete strength of 21 MPa

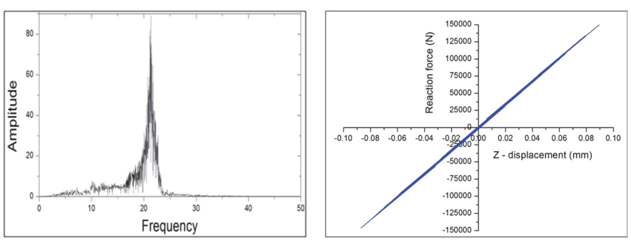

(a) FFT result (b) Load-displacement curve

Fig. 9 Results of seismic analysis for phase load RUN-2 on a concrete strength of 21 MPa

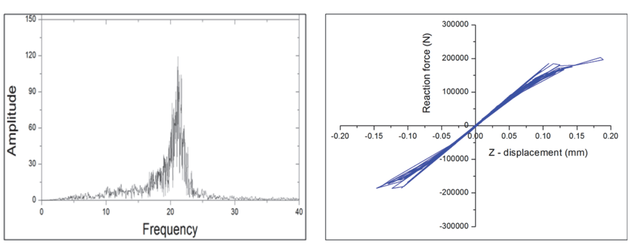

(a) FFT result (b) Load-displacement curve

Fig. 10 Results of seismic analysis for phase load RUN-3 on a concrete strength of 21 MPa

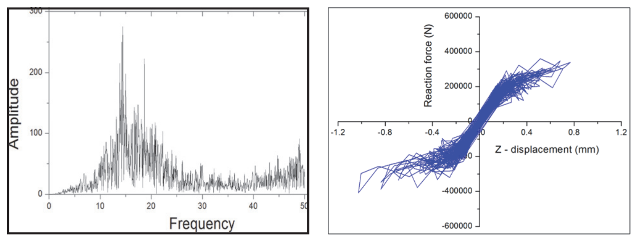

(a) FFT result (b) Load-displacement curve

Fig. 11 Results of seismic analysis for phase load RUN-4 on a concrete strength of 21 MPa

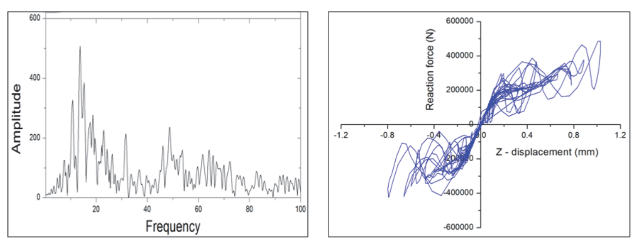

(a) FFT result (b) Load-displacement curve

Fig. 12 Results of seismic analysis for phase load RUN-5 on a concrete strength of 21 MPa

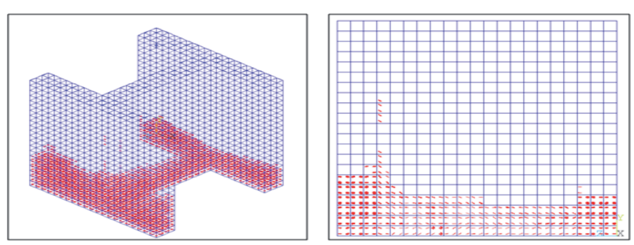

Isometric view Side view of the shear wall plan

Fig. 13 Cracking pattern for phase load RUN-4 for a concrete strength of 21 MPa

In the case of RUN-4 with a PGA of 0.5 g, as shown in Fig. 13, cracks generated at the bottom of the shear wall and flange expanded upwards. Consequently, the energy loss and stiffness reduction according to the cyclic loading history in the load-displacement curve were clearly induced by the concrete cracking. Additionally, in the case of RUN-4, the maximum load was about 0.35 MN, which was higher than the first cracking load of 0.294 MN and approached the local maximum load of 0.339 MN in the static loading case.

In the case of RUN-5 with a PGA of 0.7 g, convergence was not created any more at 3.8 seconds after the start of the time history analysis. As shown in Fig. 14, concrete cracks were distributed in a longitudinal direction below the middle of the shear wall and flange, and accordingly, energy loss and stiffness reduction clearly occurred according to the cyclic loading history. In the case of RUN-5, the maximum load at failure was 0.42 MN, and the failure occurred at a load very similar to 0.428 MN which is the failure load for the static loading case. Therefore, it is estimated that the ultimate earthquake acceleration, where a failure in the target shear wall occurs, is about 0.5 to 0.7 g.

Table 1 shows the frequencies at the maximum acceleration responses derived from the FFT for the time history of the acceleration response at the top of the shear wall by each phase of the seismic load.

In the case of the input motions with a PGA of 0.1 and 0.2 g

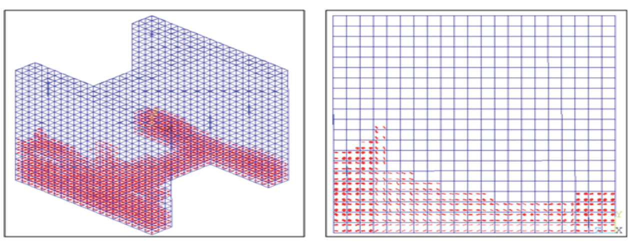

Isometric view   Side view of the shear wall plan

Fig. 14 Cracking pattern for phase load RUN-5 for a concrete strength of 21 MPa

Table 1 Frequency results

Increasing load cases	Frequency at the peak response in the FFT of the acceleration response
Modal Analysis	22.57 Hz
Run-1 (0.1 g)	21.38 Hz
Run-2 (0.2 g)	21.37 Hz
Run-3 (0.3 g)	21.17 Hz
Run-4 (0.5 g)	14.42 Hz
Run-5 (0.7 g) (Failure)	13.68 Hz

in which energy dissipation was hardly caused by concrete cracking, the frequency was about 21.4 Hz, and in the case of an input motion with a PGA of 0.3 g for which energy loss and stiffness reduction were produced by cracks at the bottom of the shear wall, the frequency at the maximum acceleration response decreased by about 0.2 Hz.

In a seismic motion with a PGA of 0.5 g for which energy loss and stiffness reduction clearly occurred due to concrete cracking at the bottom of the shear wall, the frequency at the maximum acceleration response was about 14.42 Hz with a remarkable decrease of about 36% compared with the modal analysis result, and it was found that the shear stiffness was reduced by about 60% compared with the no-cracked sound structure. In the case of the input motion with a PGA of 0.7 g at which the analysis abruptly stopped because of the occurrence of failure during the analysis, the frequency at the maximum acceleration response was 13.68 Hz, which implies about a 63% reduction in the shear stiffness compared with no-damaged shear wall.

4. Conclusions

This study was conducted to evaluate the influence of stiffness reduction in a concrete shear wall caused by cracks. The study results are summarized as follows:

(1) From the results of the nonlinear analysis of a gradual increase in the seismic load, it was found that as the magnitude of a seismic load became large, shear cracks occurred and progressed in the concrete shear wall and that energy loss and shear cracks clearly occurred according to the cyclic history.

(2) For the increasing seismic load cases, as the magnitude of the seismic load approached the ultimate seismic capacity of the shear wall, the frequency decreased by about 36% compared to the intact state, and shear stiffness decreased by about 60% compared to the crack-free sound state.

(3) It was found that in cases where concrete cracks occurred in the shear wall due to a seismic load, an considerable stiffness reduction occurred compared with the virgin load case, and it is suggested that the effect of concrete cracks in shear walls on the shear stiffness should be appropriately considered in the seismic design of shear walls.

Acknowledgments

This work was supported by Korea Institute of Nuclear Safety(KINS).

References

1. ACI 349. (2001). Code Requirements for Nuclear Safety-related Concrete Structures and Commentary. American Concrete Institute, Michigan.
2. Arel, H. Ş., Aydin, E., and Kore, S. D. (2017), Ageing management and life extension of concrete in nuclear power plants. Powder Technology, 321, 390-408.
3. ASCE/SEI 43. (2005), Seismic Design Criteria for Structures, Systems and Components in Nuclear Facilities. American Society of Civil Engineers and Structural Engineering Institute, Virginia.
4. Choubey, R. K., Kumar, S., and Rao, M. C. (2014), Effect of shear-span/depth ratio on cohesive crack and double-K fracture parameters of concrete, Advances in concrete construction, 2(3), 229-247.
5. DCD. (2011), Design control document for the AP1000. U.S. Nuclear Regulatory Commission, Washington, DC.
6. Habasaki, A., Nishikawa, T., Takiguchi, K., Kitada, Y., and Torita, H. (1999), Multi-Axial Loading Test for RC Wall of Reactor Building. SMiRT-15, H03/3, VI-107-114.
7. Hiroshi, T., Yoshio, K., Takao, N., Katsuki, T., Hideyoshi, W., and Takeyoshi, K. (2001), Multi-Axis Loading Test on RC Shear Walls Overview and Outline of Two Directional Horizontal Loading Test. Transactions on SMiRT 16, Washington, DC.
8. Kusama, K., Suzuki, A., Fukuda, R., Hirotani, T., and Takiguchi, K. (2003). Simulation Analysis of Shaking Table Test for RC Seismic Shear Wall in Multi-Axis Loading Tests. SMiRT 17, Prague, Czech Republic.
9. Mistri, A., Davis, R., and Sarkar, P. (2016), Condition assessment of fire affected reinforced concrete shear wall building–A case study. Advances in concrete construction, 4(2), 89-105.
10. NUREG/CR-6926. (2007), Evaluation of the Seismic Design Criteria in ASCE/SEI Standard 43-05 for Application to Nuclear Power Plants. U.S. Nuclear Regulatory Commission.
11. Shojaei, F., and Behnam, B. (2017), Seismic vulnerability assessment of low-rise irregular reinforced concrete structures using cumulative damage index, Advances in concrete construction, 5(4), 407-422.
12. Sogbossi, H., Verdier, J., and Multon, S. (2017), Impact of reinforcement-concrete interfaces and cracking on gas transfer in concrete. Construction and Building Materials, 157, 521-533.
13. Syed, S., and Gupta, A. (2015), Seismic fragility of RC shear walls in nuclear power plant part 2: Influence of uncertainty in material parameters on fragility of concrete shear walls. Nuclear Engineering and Design, 295, 587-596.
14. Torita, H., Matsumoto, R., Kitada, Y., Kusama, K., and Nishikawa, T. (2004), Shaking table test of RC box-type shear wall in multi-axes loading. In: 13th World Conference on Earthquake Engineering, Vancouver, BC, Canada.
15. US-APWR. (2011), Design document. Seismic Design Bases of the US-APWR Standard Plant. MUAP-10001, Rev. 4, Mitsubishi Heavy Industries, Ltd.
16. Wang, S. (2018), Analytical evaluation of the dome-cylinder interface of nuclear concrete containment subjected to internal pressure and thermal load. Engineering Structures, 161, 1-7.
17. Zhou, Y., Xu, B., Pang, R., Zou, D., and Kong, X. (2018), Stochastic seismic response and stability reliability analysis of a vertical retaining wall in front of the pumping station of a nuclear power plant using the probability density evolution method. Nuclear Engineering and Design, 334, 110-120.

Received : 03/14/2022
Revised : 04/08/2022
Accepted : 05/10/2022

요　　지 : 본 연구는 균열에 의한 콘크리트 전단벽 강성저하 영향 평가를 위해 수행되었으며, 극한 내지진 하중의 60%까지 재하한 비선형 해석 결과, 사전 균열효과에 의해 비손상 대비 진동수의 12%정도 진동수가 감소하였으며 강성 측면에서 23%정도의 감소현상을 나타냈다. 단계적으로 지진하중의 크기를 증가시킨 비선형 해석 결과, 지진하중의 세기가 커짐에 따라 콘크리트 전단벽체에 전단균열이 발생하여 진전함을 파악하고, 반복이력에 의한 에너지 손실과 강성 저하가 뚜렷하게 발생함을 알 수 있었다. 또한 두 가지 콘크리트 강도와 전단벽 제원에 대하여 지진하중의 크기가 극한 내지진 하중에 근접함에 따라 진동수의 감소량은 비손상 대비 10~40%정도로 나타났으며, 강성의 경우 비손상 대비 40%정도 수준까지 감소할 수 있는 것으로 나타났다.

핵심용어 : 지진하중, 철근콘크리트, 전단벽, 유한요소해석, 콘크리트 균열